

- (25) (a) R. E. Connick and J. W. Neely, *J. Am. Chem. Soc.*, **94**, 3419, 8646 (1972); (b) G. Liu, reported by D. P. Rablen, H. W. Dodgen, and J. P. Hunt, *Inorg. Chem.*, **15**, 931 (1976).
- (26) F. Basolo and R. G. Pearson, "Mechanisms of Inorganic Reactions", 2nd ed. Wiley, New York, N.Y., 1967, p 145.
- (27) A. L. Companion, *J. Phys. Chem.*, **73**, 739 (1969).
- (28) K. Breitschwerdt, *Ber. Bunsenges. Phys. Chem.*, **72**, 1046 (1968).
- (29) N. S. Angerman and R. B. Jordan, *Inorg. Chem.*, **8**, 2579 (1969).
- (30) C. H. Langford and T. R. Stengle, *Annu. Rev. Phys. Chem.*, **19**, 193 (1968).
- (31) F. Dickert, H. Hoffmann, and T. Janjic, *Ber. Bunsenges. Phys. Chem.*, **78**, 712 (1974).
- (32) V. Gutmann and R. Schmid, *Coord. Chem. Rev.*, **12**, 263 (1974).
- (33) R. S. Drago, *Inorg. Chem.*, **12**, 2211 (1973), and references therein.
- (34) M. Tanaka, *Inorg. Chem.*, **15**, 2325 (1976).
- (35) E. F. Caldin and H. P. Bennetto, *J. Solution Chem.*, **2**, 217 (1973).
- (36) C. H. Langford, J. P. K. Tong, and A. Merbach, *Can. J. Chem.*, **53**, 702 (1975).
- (37) W. D. Perry, R. S. Drago, and N. K. Kildahl, *J. Coord. Chem.*, **3**, 203 (1973).

Contribution from the Nuclear Research Center
"Demokritos", Athens, Greece

Mössbauer Quadrupole Splitting Analysis of Iron(IV) Dithio Chelates

V. PETROULEAS¹ and D. PETRIDIS*

Received October 16, 1976

AIC60752B

A method for the analysis of temperature-dependent quadrupole splittings in iron(IV) dithio chelates is described. The method employs a general crystal field Hamiltonian including terms of octahedral, trigonal, and C_2 symmetry. The parameters derived from the analysis point to nearly identical crystal field surroundings corresponding to a geometry between the octahedral and trigonal-prismatic limits in agreement with the known structure of one of the compounds. It is suggested that the increase of quadrupole splitting at low temperatures may be used as a marker of the above molecular symmetry. The nearly identical isomer shifts at various temperatures constitute further evidence that the compounds have similar structures and bonding properties. An important conclusion of the analysis is that the electronic properties of these iron(IV) dithio chelates are successfully interpreted on the basis of a $3d^4$ electronic configuration with some covalent character present.

Introduction

The existence of synthetic iron complexes in the formal oxidation state four is now well documented by a variety of physical methods.²⁻⁶ Apart from the diarsine complexes of the type $[\text{Fe}(\text{diars})_2\text{X}_2](\text{BF}_4)_2$,⁷ where $\text{X} = \text{Cl}$ or Br and diars = *o*-phenylenebis(dimethylarsine), all other well-characterized iron(IV) complexes bear the FeS_6 core in which the sulfur atoms belong to a dithiocarbamate group² or to the 1,1-dicarboethoxy-2,2-ethylenedithiolate dianion (DED^{2-}).³ Furthermore, there exists evidence that iron(IV) centers are present in the oxidized forms of certain peroxidases.^{8,9} Thus, the study of chemical and physical properties of synthetic iron(IV) complexes is of particular importance in order to understand the action of iron(IV) in biological systems.

Magnetic susceptibility measurements on synthetic iron(IV) complexes have yielded magnetic moments in the range 2.9–3.4 μ_B consistent with a $3d^4$ configuration in an $S = 1$ ground state. Mössbauer isomer shifts have proved very useful for assigning formal oxidation states of iron. In the case of iron(IV) complexes isomer shifts fall in the range 0.1–0.2 mm/s at room temperature relative to the metal iron. They are lower than those of iron(III) compounds in agreement with the removal of one 3d electron on passing from Fe(III) (d^5) to Fe(IV) (d^4). Quadrupole splittings (QS), on the other hand, depend upon the exact symmetry at the iron and vary in general with temperature.²

The molecular structures reported for two Fe(IV) complexes, namely, $(\text{BzPh}_3\text{P})_2[\text{Fe}(\text{DED})_3]$, I,³ and $[\text{Fe}(\text{pyrrdtc})_3](\text{ClO}_4)$, II,⁴ are severely distorted from octahedral coordination. The average projected twist angle of the two triangular faces of the FeS_6 unit can be taken as an indication of the deviation from octahedral geometry. In this way, the values of 35.9 and 38°, reported for compounds I and II, lie between the extremes of 60° corresponding to octahedral and 0° corresponding to trigonal-prismatic geometry. However, it must be emphasized that the above values represent an average over three greatly different projected twist angles each

corresponding to one of the three sulfur chelating ligands. Martin and Takats have pointed out the similarity in the structures of compound I and of tetraphenylarsonium tris-(benzenedithiolato)tantalate(V).¹⁰ For the latter compound the symmetry at the tantalum atom is best described as originating from a trigonal prism which suffers individual rotations of the chelating ligands around the C_2 axis. One of these rotations, however, is more severe than the other two causing a lowering of the overall symmetry to C_2 .

Recently, detailed ligand field analysis of the Mössbauer spectra of I has shown that the temperature variation of QS is well accounted for by ascribing to the complex a geometry close to a trigonal prism with an exact C_2 point symmetry.¹¹ In particular, the small increase of the QS at 4.2 K relative to the value at 77 K was found to be a unique feature of the above-described asymmetric type of distortion. In the present work we have extended the QS analysis to certain tris(dithiocarbamato)iron(IV) complexes with the purpose of determining whether they behave similarly to I and more particularly to correlate QS data with structural characteristics of analogous compounds.

Experimental Section

The iron(IV) perchlorates $[\text{Fe}(\text{pyrrdtc})_3]\text{ClO}_4$, II, and $[\text{Fe}(\text{S}_2\text{CNMe}_2)_3]\text{ClO}_4$, IV, were prepared according to Golding et al.,¹² the tetrafluoroborates $[\text{Fe}(\text{S}_2\text{CNEt}_2)_3]\text{BF}_4$, III, and $[\text{Fe}(\text{pyrrdtc})_3]\text{BF}_4$, V, were prepared following the method of Pasek and Straub² except that the boron trifluoride was replaced by a 48% $\text{BF}_3\cdot\text{Et}_2\text{O}$ solution. The products were recrystallized twice from dichloromethane–benzene. Their identity was confirmed from Mössbauer and infrared spectra. Mössbauer spectra were recorded with a conventional constant-acceleration spectrometer as described before.¹³ The source was 30 mCi of ^{57}Co in an Rh matrix. The system was calibrated with an iron-foil absorber. Measurements at 4.2 K and lower temperatures were made using a liquid helium cryostat and vapor pressure techniques. The temperature range 56–300 K was covered in a liquid nitrogen cryostat either by vapor pressure techniques or by means of a heater attached to the sample holder. Relative errors within each set of QS data were ± 0.004 mm/s. By repeating the room-temperature, liquid nitrogen,

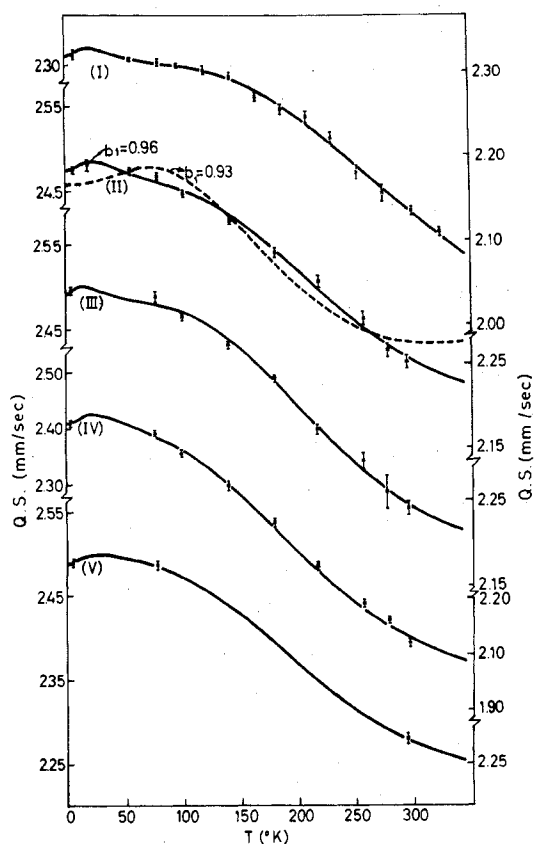


Figure 1. Temperature variation of the quadrupole splitting in compounds I-V. Solid lines are computer fits obtained by using the ligand field model described in the text.

and liquid helium measurements at different periods an overall error of ± 0.01 mm/s was established.

Results and Analysis

The Mössbauer spectra of the complexes comprise well-defined quadrupole doublets. Values of isomer shift and quadrupole splitting at various temperatures are listed in Table

Table I. Mössbauer Results of Iron(IV) Dithio Chelates

| Compd | 297 K | | 77.3 K | | 4.2 K | |
|----------------|-----------|------------------|-----------|------------------|-----------|------------------|
| | QS, mm/s | $\delta,^a$ mm/s | QS, mm/s | $\delta,^a$ mm/s | QS, mm/s | $\delta,^a$ mm/s |
| I ^b | 2.132 (5) | 0.19 (1) | 2.306 (4) | 0.30 (1) | 2.313 (5) | 0.30 (1) |
| II | 2.251 (8) | 0.19 (1) | 2.469 (3) | 0.30 (1) | 2.475 (4) | 0.31 (1) |
| III | 2.241 (8) | 0.19 (1) | 2.490 (6) | 0.30 (1) | 2.496 (4) | 0.31 (1) |
| IV | 2.02 (1) | 0.19 (1) | 2.390 (4) | 0.29 (1) | 2.408 (4) | 0.30 (1) |
| V | 2.277 (6) | 0.19 (1) | 2.486 (4) | 0.30 (1) | 2.486 (4) | 0.30 (1) |

^a Relative to iron at room temperature. ^b From ref 10.

I. The values at 77 and 290 K agree well with those previously reported.^{2,12} The variation of quadrupole splittings with temperature together with theoretical fits is shown in Figure 1.

The first detailed Mössbauer analysis of iron(IV) complexes was reported by Paez et al.¹⁴ on *trans*-[Fe(diars)₂X₂](BF₄)₂, X = Cl, Br. The quadrupole splittings were found nearly constant between 298 and 4.2 K, though the experimental errors were rather large. Spectra were also taken in the presence of a large external magnetic field and were interpreted in terms of a spin Hamiltonian with an effective spin $S = 1$. By contrast to the iron(IV) diarsine complexes the quadrupole splittings of iron(IV) dithiocarbamates and (BzPh₃P)₂[Fe(DED₂)] vary significantly with temperature. The spectra, however, in an applied magnetic field exhibit a nearly "diamagnetic" behavior similar to that observed in the diarsine complexes. Recently, ligand field theory was successfully employed for the analysis of QS data and magnetically perturbed spectra of I.¹¹ A similar analysis is now applied to the four (II-V) iron(IV)dithiocarbamates.

The Hamiltonian used for the calculation is

$$\mathcal{H} = \mathcal{H}_0 + V_0 + V_T + \mathcal{H}_C + V_{C_2} + \zeta \sum_{i=1}^4 l_i \cdot s_i \quad (1)$$

where \mathcal{H}_0 represents the free-ion kinetic and potential energy of spherical symmetry, \mathcal{H}_C is the Coulomb repulsion between the four 3d electrons, the last term represents the l-s coupling, and the various V terms account for the unusual geometry at the iron site described in the Introduction. The effect of these V terms is illustrated in Figure 2, where a possible correlation

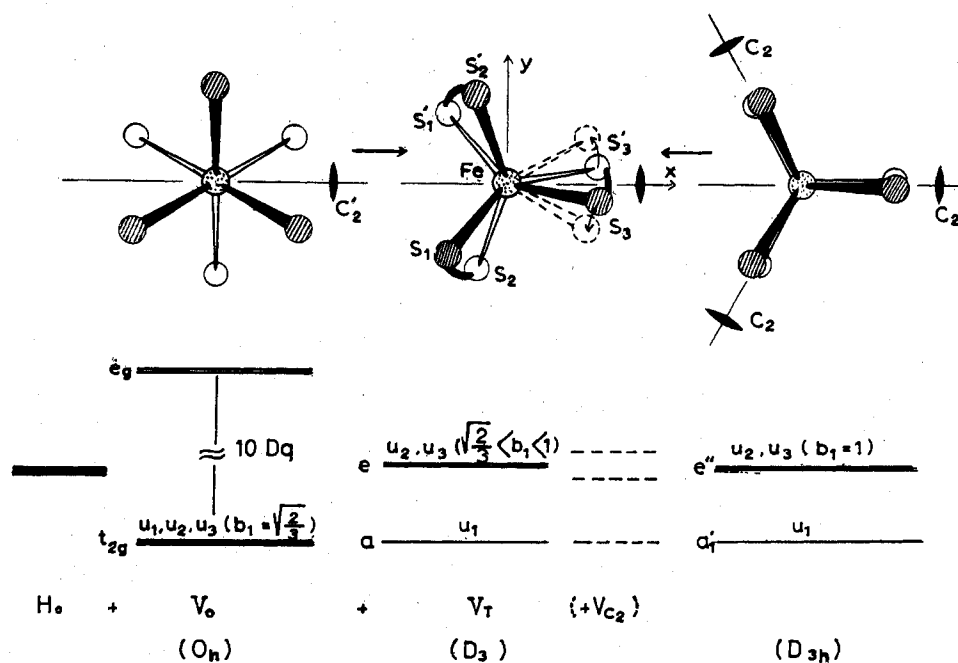


Figure 2. Idealized diagram depicting how the actual arrangement of the FeS₄ core may be reached from either the octahedral or the trigonal-prismatic geometry. A schematic correlation diagram of the single 3d-electron crystal field eigenstates is also shown (from ref 10).

Table II. Values of Crystal Field and Quadrupole Splitting Parameters Derived from Present Analysis

| Compd | Δ_1, cm^{-1} | Δ_2, cm^{-1} | ζ, cm^{-1} | b_1 | c_1 | $\Delta E_0, \text{mm/s}$ | $\Delta E_{\text{lat}}, \text{mm/s}$ |
|----------------|----------------------------|----------------------------|-------------------------|-----------|----------|---------------------------|--------------------------------------|
| I ^a | 650 ± 75 | 700 ± 75 | 300 ± 50 | 0.960 (5) | 0.92 (3) | 2.9 (4) | 0.0 (3) |
| II | 550 ± 50 | 600 ± 50 | 340 ± 50 | 0.960 (5) | 0.92 (3) | 2.6 (3) | 0.3 (3) |
| III | 575 ± 75 | 600 ± 75 | 330 ± 50 | 0.960 (5) | 0.92 (3) | 3.0 (5) | 0.0 (4) |
| IV | 550 ± 75 | 450 ± 75 | 350 ± 50 | 0.958 (5) | 0.92 (3) | 3.1 (3) | -0.2 (2) |
| V | 600 | 600 | 350 | 0.96 | 0.92 | 3.0 | |

^a From ref 10.

between the FeS_6 polyhedron (compounds I and II) and the extremes of octahedral and trigonal-prismatic arrangement is also shown. In this way, the octahedral term V_0 produces the familiar pattern of splitting of the d orbitals into the t_{2g} and e_g states. The next term V_T , which describes a twist around the C_3 axis, lifts in part the degeneracy of the t_{2g} orbitals and mixes them with the higher e_g orbitals. By using group theoretical arguments it can be shown that the three lowest single-electron eigenfunctions of the first three terms in (1) are expressed by the following combinations of the familiar octahedral wave functions

$$\begin{aligned} u_1 &= d_{z^2} \\ u_2 &= b_1 d_{xy} + b_2 d_{x^2-y^2} \\ u_3 &= b_1 d_{x^2-y^2} + b_2 d_{yz}, \quad b_1^2 + b_2^2 = 1 \end{aligned} \quad (2)$$

where the z axis is chosen along the C_3 axis and the x axis along the C_2' axis of the octahedron (Figure 2). The b 's are mixing coefficients, which assume the values $b_1 = (2/3)^{1/2}$, $b_2 = (1/3)^{1/2}$ for octahedral symmetry (O_h)¹⁵ and $b_1 = 1$, $b_2 = 0$ for trigonal prismatic (D_{3h}). Values of b_1 between these two extremes account for intermediate distortions.

We next proceed to construct from (2) the $S = 1$ Slater determinants. We designate them by $U_{i,m}$, where $i = 1, 2, 3$ specifies the orbital character of the function and $m = -1, 0, 1$ stands for the z component of the total spin, e.g., $U_{2,1} = |u_1^+ u_2^+ u_3^+ u_2^-|$, $U_{2,0} = (1/2^{1/2})\{|u_1^+ u_2^+ u_3^+ u_2^-| + |u_1^+ u_2^+ u_3^- u_2^+|\}$, etc. Using these four electron wave functions we calculate the interelectronic repulsion energies. The main effect of the \mathcal{H}_C term is to stabilize an $S = 1$ ground state and furthermore to increase or decrease the energy separation due to V_T without mixing the states or lifting the degeneracy.

The next symmetry term (C_2) lifts completely the orbital degeneracy and induces mixing of the levels $U_{1,m}$ and $U_{3,m}$ ($m = -1, 0, 1$) which is described in terms of the adjustable parameters c_1 and c_3 ($c_1^2 + c_3^2 = 1$). To summarize, the eigenstates of (1), except for the last term, are described in terms of the four-electron ($S = 1$) determinant wave functions

$$\begin{aligned} U'_{1,m} &= c_1 U_{1,m} + c_3 U_{3,m} \\ U'_{2,m} &= U_{2,m} \\ U'_{3,m} &= -c_3 U_{1,m} + c_1 U_{3,m}, \quad c_1^2 + c_3^2 = 1 \end{aligned} \quad (3)$$

at energies 0, Δ_1 , and Δ_2 , respectively.

Finally, the matrix elements of the l-s coupling term in (1) are calculated in terms of the basis $U_{i,m}$ using operator techniques.

Diagonalization of the 9×9 matrix of the Hamiltonian (1) leads to the determination of the eigenfunctions Ψ_i ($i = 1 \dots 9$) and eigenvalues E_i ($i = 1 \dots 9$). In our analysis the mixing coefficients b_1 and c_1 , the energy separations Δ_1 and Δ_2 , and the spin-orbit coupling constant ζ are treated as adjustable parameters. The eigenvalues obtained in this way are in turn used to obtain the expectation values of the components of the electric field gradient using operator techniques. The quadrupole splitting is calculated by means of the relation¹⁶

$$\Delta E_Q = (\Delta E_0)(F(T)) + \Delta E_{\text{lat}} \quad (4)$$

where $\Delta E_0 = (2/7)e^2Q(1-R)\langle r^{-3} \rangle_{3d}$, ΔE_{lat} is the tempera-

ture-independent contribution of the lattice to QS, and $F(T)$ is a function of the thermal averages of the lower eigenstates and varies therefore with Δ_1 , Δ_2 , ζ , b_1 , and c_1 . Explicitly, the function $F(T)$ is given by

$$\begin{aligned} F(T) &= \{(\langle V_{zz} \rangle_{\text{av}})^2 + 1/3(\langle V_{xx} - V_{yy} \rangle_{\text{av}})^2 \\ &\quad + 4/3[(\langle V_{xy} \rangle_{\text{av}})^2 + (\langle V_{yz} \rangle_{\text{av}})^2 + (\langle V_{zx} \rangle_{\text{av}})^2]\}^{1/2} \end{aligned}$$

where

$$\langle V_{ij} \rangle_{\text{av}} = \frac{\sum \langle V_{ij} \rangle_n \exp(-E_n/kT)}{\sum \exp(-E_n/kT)}$$

with n running over the nine eigenstates of (1).

In order to fit eq 4 to the experimental results a program was written which diagonalizes (1) and calculates $F(T)$ for each set of the adjustable parameters. The constants ΔE_0 and U are then adjusted by linear least-squares fitting to the experimental data. This calculation is repeated for all probable sets of the parameters Δ_1 , Δ_2 , ζ , b_1 , and c_1 ; the set which minimizes the parameter

$$\sigma^2 = \sum_i \frac{(\text{QS}_i^{\text{theor}} - \text{QS}_i^{\text{exptl}})^2}{(\Delta Q_i^{\text{exptl}})^2}$$

is then selected.¹⁶ The best theoretical simulations to the experimental results gave for compounds II-V the values listed in Table II in which the analogous values of I are also shown for comparison reasons. These values were used for the calculation of the theoretical QS vs. T curves shown together with the experimental data in Figure 1. The curves account well for all the details of QS variation. The narrow maximum near liquid helium temperatures appearing in all theoretical curves has been detected rather positively, as indicated by the QS value at 18 K in Figure 1 (II).

Discussion

Examination of the results in Table II shows that all five compounds have effectively similar crystal field and quadrupole splitting parameters. Thus, Δ_1 and Δ_2 lie near 600 cm^{-1} while ζ has a value close to 350 cm^{-1} . The latter appears decreased by about 30% from the free-ion value of $\sim 500 \text{ cm}^{-1}$.¹⁷ A similar decrease has been observed in many ferrous compounds¹⁸ and is generally attributed to radial expansion or to overlap with the ligand orbitals. To which extent each of the above factors contributes to the observed decrease is not easily determined and requires more data and more elaborate calculations. An additional source of information concerning covalency effects is the bare quadrupole constant ΔE_0 , which was found here close to 3.0 mm/s . Unfortunately, data for the calculation of ΔE_0 for the free Fe(IV) ion are not presently available, whereas experimental ΔE_0 values for ionic Fe(IV) compounds have not been reported. Assuming, however, that ζ and ΔE_0 are roughly equally decreased owing to covalency, we arrive at an estimate of $\Delta E_0 \approx 4.5 \text{ mm/s}$ for the free Fe(IV) ion. Finally, additional evidence that all five compounds have similar covalency is the nearly equal isomer shift values in Table I. Moreover, the similar temperature dependence of the isomer shifts implies similar modes of vibrations of the Fe(IV) ion.

An important result of the analysis is the high sensitivity of QS to the trigonal distortion parameter b_1 . This effect is illustrated in Figure 1 (II), where the solid curve represents the best fit to the data with $b_1 = 0.96$ whereas the dotted line is the best simulation obtained with b_1 fixed to 0.93. The latter curve exhibits a broad maximum and then drops appreciably at 4.2 K. This behavior becomes more pronounced as one approaches octahedral symmetry for which $b_1 = 0.816$. We therefore conclude that an increase or at least a constant value of QS at liquid helium temperature relative to the value at liquid nitrogen temperature may be used as a diagnostic feature for a symmetry intermediate between the octahedral and trigonal-prismatic limits, provided that the room-temperature value is substantially lower.

The variation of the QS with temperature is influenced to a lesser extent by the parameter c_1 which we take as a measure of the C_2 distortion. Although the range of values of c_2 is not so narrow as that for b_1 , we have found that the QS behavior cannot be accounted for by omitting the C_2 distortion.

The similar thermal dependence of the quadrupole splittings as well as the very close crystal field parameters and the almost identical isomer shifts between I and the iron(IV) dithiocarbamates suggests that the structural characteristics and the detailed nature of iron bonding in these two classes of iron(IV) compounds are very similar. This is confirmed by the nearly identical structures of I and II. The same arguments lead to the conclusion that the exact environment at the iron is also similar in compounds II-V. Finally, we remark that the successful interpretation of Mössbauer data by a method based on ligand field theory offers substantial support to the fact that

in these FeS_6 compounds we are concerned with iron in a well-established +4 oxidation level.

Registry No. II, 39838-28-3; III, 35270-33-8; IV, 39838-24-9; V, 35270-36-1.

References and Notes

- (1) National Research Foundation Fellow.
- (2) E. A. Pasek and D. K. Straub, *Inorg. Chem.*, **11**, 259 (1972).
- (3) F. J. Hollander, R. Pedelty, and D. Coucouvanis, *J. Am. Chem. Soc.*, **96**, 4032 (1974).
- (4) R. L. Martin, N. M. Rohde, G. B. Robertson, and D. Taylor, *J. Am. Chem. Soc.*, **96**, 3647 (1974).
- (5) R. Chant, A. R. Hendrickson, R. L. Martin, and N. M. Rohde, *Aust. J. Chem.*, **26**, 2533 (1973).
- (6) G. Cauquis and L. Lachenal, *Inorg. Nucl. Chem. Lett.*, **9**, 1095 (1973).
- (7) G. S. F. Hazeldean, R. S. Nyholm, and R. V. Pavish, *J. Chem. Soc.*, **4**, 162 (1966).
- (8) T. H. Moss, A. Ehrenberg, and A. J. Bearden, *Biochemistry*, **8**, 4159 (1969).
- (9) R. H. Felton, G. S. Owen, D. Dolphin, and J. Fajer, *J. Am. Chem. Soc.*, **93**, 6332 (1971).
- (10) J. L. Martin and J. Takats, *Inorg. Chem.*, **14**, 1358 (1975).
- (11) V. Petrouleas, A. Kostikas, A. Simopoulos, and D. Coucouvanis, *J. Phys.*, **37**, Colloque C6, 507 (1976).
- (12) R. M. Golding, C. M. Harris, K. J. Jessop, and W. C. Tennant, *Aust. J. Chem.*, **25**, 2567 (1972).
- (13) N. H. Gangas, N. Gaitanis, A. Kostikas, and A. Simopoulos, *Nucl. Instrum. Methods*, **106**, 409 (1973).
- (14) E. A. Paez, D. L. Weaver, and W. T. Oosterhuis, *J. Chem. Phys.*, **57**, 3709 (1972).
- (15) C. J. Ballhausen, "Introduction to Ligand Field Theory", McGraw-Hill, New York, N.Y., 1962, p 68.
- (16) V. Petrouleas, A. Kostikas, and A. Simopoulos, *Phys. Rev. B*, **12**, 4666 (1975).
- (17) B. N. Figgis, "Introduction to Ligand Fields", Wiley, New York, N.Y., 1966.
- (18) For a review on ferrous compounds data see F. Varret, *J. Phys.*, **37**, Colloque C6, 481 (1976).

Contribution from the Department of Chemistry,
Massachusetts Institute of Technology, Cambridge, Massachusetts 02139

Photooxidation of a Tetranuclear Cluster Complex in the Presence of Halocarbons. Photochemistry of the Carbonyl(η^5 -cyclopentadienyl)iron(I) Tetramer

C. RANDOLPH BOCK and MARK S. WRIGHTON*¹

Received November 5, 1976

AIC608035

The photochemistry and electronic absorption spectra of $[(\eta^5-C_5H_5)Fe(CO)]_4$ in the presence of halocarbons are reported. Irradiation of the complex at the appropriate wavelengths results in photooxidation, giving initially quantitative yields of $[(\eta^5-C_5H_5)Fe(CO)]_4^+$. This is the only photoreaction observed for any irradiation wavelength longer than 300 nm. In the absence of charge-acceptor solvents no photooxidation is found: the complex is photoinert in either benzene or CH_3CN . The quantum efficiency in the presence of halocarbons depends on cosolvent, the halocarbon, and wavelength. For example, in 1:1 $CH_3CN-CCl_4$ (by volume) the initial quantum yields are 0.21 at 313 nm, 0.03 at 366 nm, 0.002 at 405 nm, and ~ 0.0005 at 436 nm. But in pure CCl_4 the 313-nm quantum yield is only 0.05. The 313-nm yield for 1:1 $CH_2Cl_2-CH_3CN$ is 0.0007. The absorption spectra reveal a halocarbon dependence in the near-UV, consistent with a charge-transfer-to-solvent excitation (CTTS). The CTTS maximum correlates with the ease of reduction of the halocarbons, and the wavelength dependence of the photooxidation substantiates the conclusion that the CTTS excitation is responsible for the photochemistry.

Introduction

Photochemical reactions of metal-metal bonded complexes have only been extensively investigated for dinuclear complexes.²⁻⁶ Some qualitative reports concern the trinuclear species $M_3(CO)_{12}$ ($M = Fe, Ru, Os$).⁶⁻¹⁰ In all of the cases studied thus far, the dominant form of excited-state chemical decay is rupture of the metal-metal bond(s) to ultimately yield mononuclear complexes. For larger clusters where one metal atom is bonded to more than one or two other metal atoms one might expect that one-electron excited states may not result in enough labilization to give photodeclusterification. Thus, ligand photosubstitution and photoredox processes may be

important and lead to new ways to modify clusters, while retaining the essential framework bonding associated with the metal-metal core.

In this report we describe the photochemical behavior of the tetranuclear cluster $[(\eta^5-C_5H_5)Fe(CO)]_4$. This species has been known¹¹ for some time and is known¹² to undergo reversible reduction and oxidation, but no photochemical studies have been reported. We have examined the photochemical behavior of the complex in the presence of potential nucleophiles which could replace CO, but we found the complex to be essentially inert to ligand substitution. We do find that $[(\eta^5-C_5H_5)Fe(CO)]_4$ can undergo photooxidation in the